AI Mix Design of Fly Ash Admixed Concrete Based on Mechanical and Environmental Impact Considerations

Kennedy C. Onyelowe [1], Ahmed M. Ebid [2*], Hisham A. Mahdi [2], Fortune K. C. Onyelowe [3], Yazdan Shafieyoon [4], Michael E. Onyia [5], Hyginus N. Onah [5]

[1] Department of Civil Engineering, School of Engineering, University of the Peloponesse, GR-26334, Patras, Greece.

[2] Department of Structural Engineering, Faculty of Engineering and Technology, Future University in Egypt, New Cairo 11865, Egypt.

[3] Department of Computer Engineering, Michael Okpara University of Agriculture, Umuahia 440109, Abia State, Nigeria.

[4] School of Railway Engineering, Iran University of Science and Technology, Tehran, Iran.

[5] Department of Civil Engineering, Faculty of Engineering, University of Nigeria, Nsukka, Nsukka, Nigeria.

Abstract

It has become very important in the field of concrete technology to develop intelligent models to reduce overdependence on laboratory studies prior to concrete infrastructure designs. In order to achieve this, a database representing the global behavior and performance of concrete mixes is collected and prepared for use. In this research work, an extensive literature search was used to collect 112 concrete mixes corresponding to fly ash and binder ratios (FA/B), coarse aggregate and binder ratios (CAg/B), fine aggregate and binder ratios (FAg/B), 28-day concrete compressive strength (Fc28), and the environmental impact point (P) estimated as a life cycle assessment of greenhouse gas emissions from fly ash- and cement-based concrete. Statistical analysis, linear regression (LNR), and artificial intelligence (AI) studies were conducted on the collected database. The material binder ratios were deployed as input variables to predict Fc28 and P as the response variables. From the collected concrete mix data, it was observed that mixes with a higher cement content produce higher compressive strengths and a higher carbon footprint impact compared to mixes with a lower amount of FA. The results of the LNR and AI modeling showed that LNR performed lower than the AI techniques, with an R^2 (SSE) of 48.1% (26.5) for Fc and 91.2% (7.9) for P. But ANN, with performance indices of 95.5% (9.4) and 99.1% (2.6) for Fc and P, respectively, outclassed EPR with 90.3% (13.9) and 97.7% (4.2) performance indices for Fc and P, respectively. Taylor's and variance diagrams were also used to study the behavior of the models for Fc28 and P compared to the measured values. The results show that the ANN and EPR models for Fc28 lie within the RMSE envelop of less than 0.5% and a standard deviation of between 15 MPa and 20 MPa, while the coefficient of determination sector lies between 95% and 99% except for LNR, which lies in the region of less than 80%. In the case of the P models, all the predicted models lie within the RMSE envelop of between 0.5% and 1.0%, a coefficient of determination sector of 95% and above, and a standard deviation between 2.0 and 3.0 points of impact. The variance between measured and modeled values shows that ANN has the best distribution, which agrees with the performance accuracy and fits. Lastly, the ANN learning ability was used to develop a mix design tool used to design sustainable concrete Fc28 based on environmental impact considerations.

Keywords: Environmental Impact; Life Cycle Assessment; Green Concrete; Greenhouses Gas Emission; Sustainable Concrete.

1. Introduction

Approximately 25 billion cubic meters of concrete are used globally as a construction material each year [1]. One of the most crucial concrete constituents is binder material, like ordinary Portland cement (OPC), which has an essential role in hydration in the concrete microstructure [2]. The cement industry is confronted with a number of challenges, including dwindling raw materials, steep increases in demand for concrete, the depletion of non-renewable resources, and environmental degradation.

Concerning greenhouse gas emissions, Portland cement production worldwide contributes about 1.35 billion tons per year, or roughly 7% of all greenhouse gas emissions in the earth's atmosphere [3]. More specifically, OPC production releases approximately 1.5 billion tons of CO_2 annually, about 9% of overall global CO_2 emissions [4]. As sustainability concerns within the construction industry have increased, it has become increasingly common to produce concrete with cement replaced with supplementary cementitious materials (SCMs). Originally, SCMs were created from waste materials or by-products generated by industries [5]. Silica fume (SF), granulated blast furnace slag (GBFS), and rice husk ash (RHA) can be used in concrete as SCMs in addition to fly ash (FA). The availability of these materials is somewhat limited in comparison to the FA. They are utilized in a wide variety of products, including blended cement [6–9], concrete batching [10–17], and concrete products [18, 19]. Consequently, sustainable construction materials are highly desired.

Fly ash (FA) is a kind of industrial waste or by-product of coal burning made up of fine fuel particles found in flue gases and coal-fired boilers [20]. FA can be classified either as Class F or Class C, according to ASTM C618 [21], depending on the amount of alumina, silica, and iron it contains: Class F if it has at least 70% of the mentioned materials and Class C if it contains 50% but less than 70%. The use of FA as a SCM in concrete could significantly lower the pollution caused by cement production by reducing CO_2 emissions [20]. Approximately 544 million tons of FA are produced worldwide annually, and 80% of them are disposed of in landfills [1, 22]. When recycled and reused, it is not discarded in landfills; therefore, it has fewer negative impacts on the environment. In order of priority, the top five applications of FA are (I) concrete and cement, (II) embankments, ash dykes, and rising roads, (III) lowland area retrieval and land-filling, (IV) bricks and blocks, and (V) mine-filling and tiles [1, 22]. The economic impact is another crucial component of sustainability, especially in mass production. Considering transportation, fly ash is generally more cost-effective than OPC and modifies the properties of concrete in both the fresh and hardened. Thus, the use of FA in place of plain concrete would be beneficial for concrete mixtures for less cost [23].

The Life Cycle Assessment (LCA) is a methodology for assessing the environmental impact of products (e.g., fly ash) and industrial processes defined by ISO 14040-14044 [24]. A sustainable solution for using fly ash in construction will require comparable performance with other commonly used building materials [25]. Seto et al. [26] developed LCA models for concrete that contain 10, 25, and 50% FA as cement replacement. FA demonstrated lower environmental impact (i.e., the Global Warming Potential Index) by up to 43% through different LCA allocation scenarios and weighting schemes. A study by Tosun-Felekoğlu et al. [27] examined the sustainability of both types of FA, Class C and Class F, for engineering cementitious composites made from high-tenacity polypropylene. Comparatively to conventional Polyvinyl Alcohol Fiber reinforced engineered cementitious composites, class F significantly reduced costs and CO_2 emissions (45% and 55%, respectively). Fly ash also has excellent potential for improving air quality [28]. Studies in recent years have shown that using FA as a SCM in infrastructure could reduce CO_2 and other pollutants, as quantified by a life cycle assessment [29–31]. It is interesting to note that Ahmaruzzaman and Gupta demonstrated that fly ash can be used as a sorbent alternative to carbon to remove gases such as NO_x, SO_x, and mercury [32].

The compressive strength (CS) of concrete is an important mechanical property that is regarded as an essential component of construction. Several factors influence the compressive strength of concrete containing FA, including the amount of FA, the water to binder ratio, and the properties of the mixture's constituents [33–35]. In addition, due to the slow rate at which FA reacts with liquid, the initial compressive strength of concrete is low; however, over time, the strength increases [36, 37]. Typically, employing fly ash in concrete varies around 15–30 percent of the cementitious binder, although to control concrete temperature rise, higher replacement levels, 30%-50%, have been utilized for large structures (e.g., foundations and dams) [25].

As an alternative, estimating the compressive strength of concrete using machine-learning predictive models can be used to select the fly ash based on the parameters mentioned earlier in an optimal way. This can be helpful in terms of time and monetary issues while also providing valuable information for scheduling activities. Pala et al. [38] investigated the influence of SF and FA replacement on concrete's strength using neural networks (NNs), demonstrating NNs as a reliable tool for assessing cementitious material's impact on concrete's CS. Chopra et al. [39] compared the Genetic Programming (GP) and Artificial Neural Network (ANN) techniques to predict concrete compressive strength without or with FA. Therefore, it can be concluded that the ANN model is the most reliable. Yuan et al. [40] found that when using Genetic Algorithms-Artificial Neural Network (GA-ANN) hybrid models to predict the compressive strength of concrete mixtures with additives like GBFS and FA, there is no need to carry out time-consuming and sophisticated laboratory tests. Also, it is more accurate and readily applicable to replace the conventional regression models and traditional Back Propagation-Artificial Neural Network (BP-ANN) models in real engineering practices.

In this study, at first, the LCA evaluation is conducted using the collected database to evaluate the concrete's environmental impact. Each concrete mixture will be evaluated for its performance, accuracy, and sensitivity using the LCA method. Second, the predictive models will be used to provide closed-form equations for 28-day compressive strength (Fc28) and environmental impact index (P), with the other parameters serving as predictors (e.g., cement, fly ash, aggregates, water, and W/B). The model techniques being considered are the traditional linear regression (TLR or LNR), the artificial neural network (ANN), and the evolutionary polynomial regression (EPR).

2. Methodology

2.1. Experimental Data Collection

An extensive literature search (experimental data, data arrangement, and tabulation), which has been conducted in this research work to collect the amount of concrete mix materials corresponding to the compressive strength at 28 days (Fc28) and the environmental impact, which has been evaluated by the method of life cycle assessment (LCA), has revealed the influence of fly ash (FA) proportion by partial or total replacement in the production of a more sustainable and eco-friendly concrete. During this first phase of the present research work, previous relevant research papers were reviewed [41–52] and data points relevant to this modeling and optimization exercise were collected and tabulated. Figure 1 shows the theoretical framework of the activities of this research work. In the second phase, statistical analysis, including Pearson's correlation and histogram charts of the variables, was conducted and presented to show the general statistical behavior and consistency between the input variables and the outputs. The third phase was focused on the general analysis of the collected data, a regression study, and AI modeling, which employed the learning abilities of the ANN and EPR. While the ANN and EPR were deployed in predicting the FA-admixed concrete compressive strength at 28 days (Fc28) and the impact of the concrete mix materials with particular emphasis on the binders (cement and FA) in the fourth phase, the smart ability of the ANN was deployed to develop a mix design tool using the same technique mentioned in Pérez-Acebo et al. [53]. The tool formulates mix designs that meet the strength and environmental impact conditions of sustainable and green concrete.

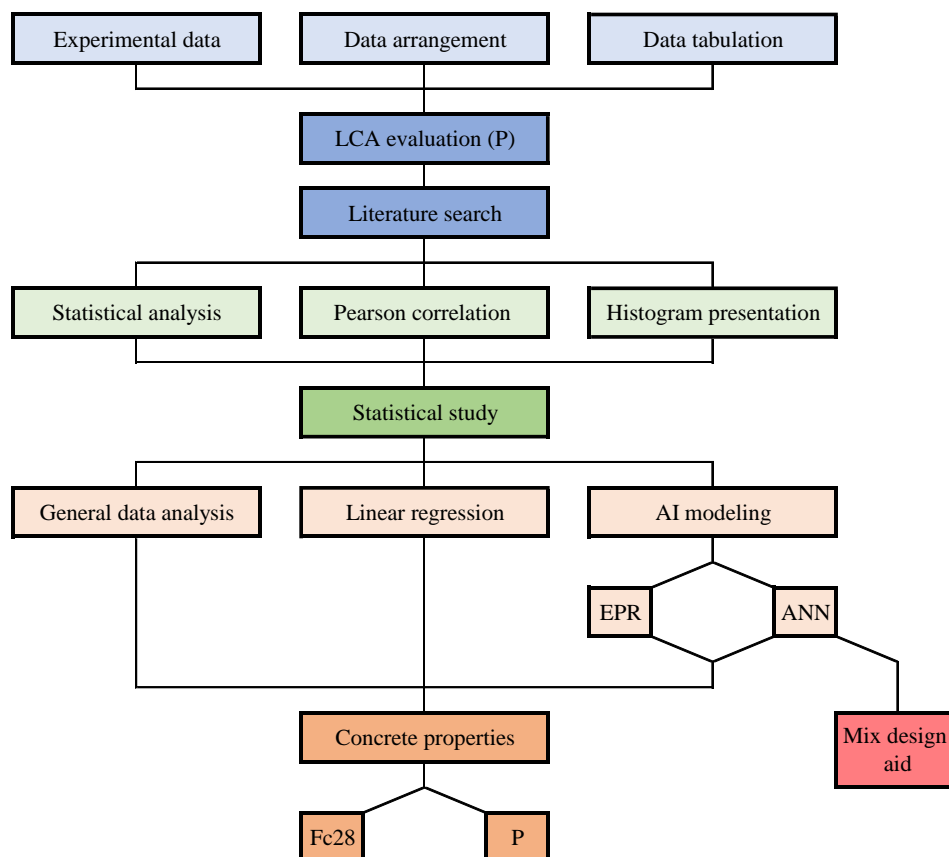**Figure 1. Theoretical framework for the 28 days concrete Fc and P data collection, modeling and AI mix design tool development**

2.2. Collected Database and Statistical Analysis

At the end of an extensive literature search, 112 records were collected from experimental tested concrete mixtures admixed with FA with different components' ratios arranged and tabulated in the appendix I. Each record contains the following data:

- Fly Ash to binder ratio (FA/B),
- Fine aggregates (Sand) to binder ratio (Fag/B),
- Coarse aggregates to binder ratio (Cag/B),
- 28 days cylinder compressive strength of concrete (Fc28) MPa,
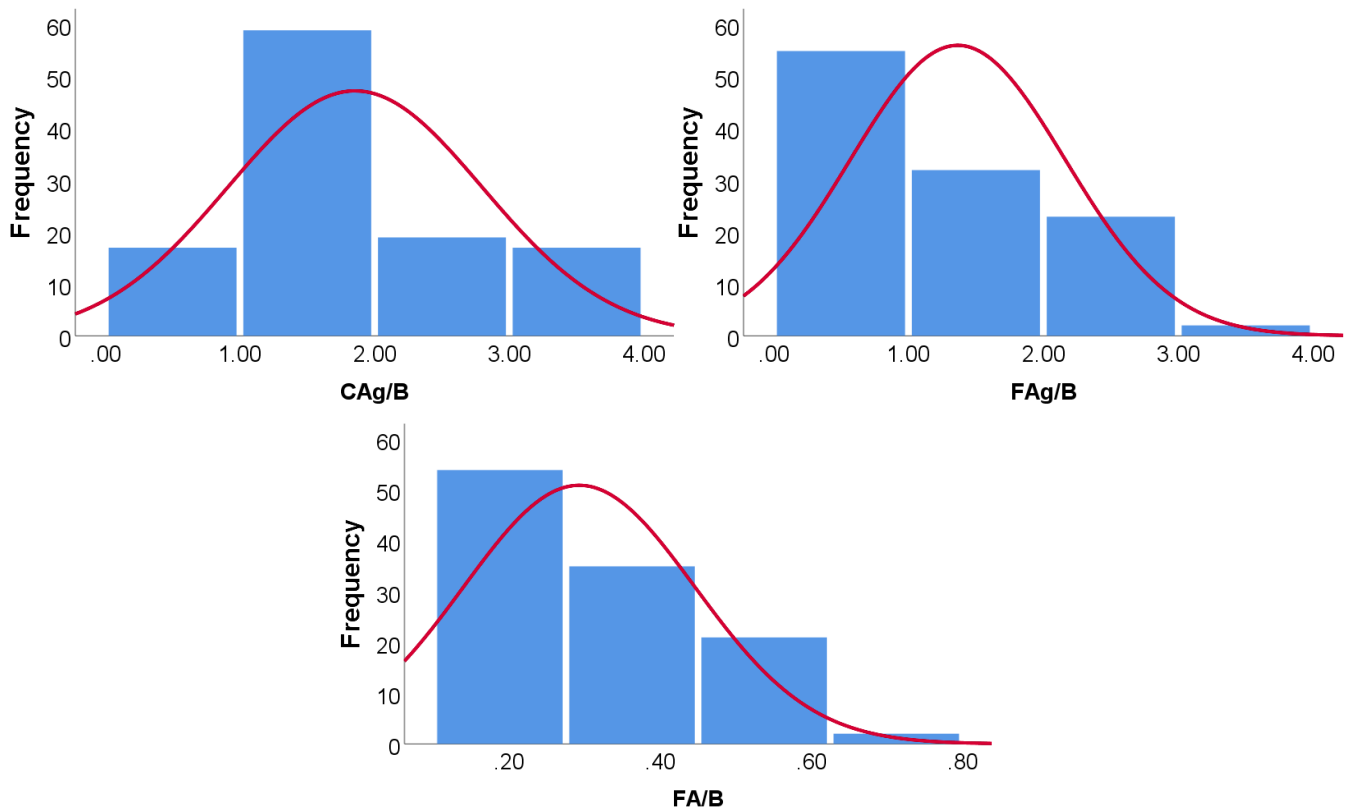- Environmental impact factor (P),

where, (B) is binder content (Cement content + Fly ash content). The collected records were divided into training set (90 records) and validation set (22 records). Tables 1 and 2 summarize their statistical characteristics and the Pearson correlation matrix, respectively. Finally, Figure 2 shows the histograms for both inputs and outputs.

Table 1. Statistical analysis of collected database

Item	FA/B	FAg/B	CAg/B	Fcu (MPa)	P
Mean	0.2925	1.3654	1.8540	32.1875	7.2777
Median	0.3000	1.0600	1.4600	35.5500	7.7000
Mode	0.13	0.83	1.98	33.00	4.00
Std. Deviation	0.15332	0.79654	0.94457	13.68721	2.03203
Variance	0.024	0.634	0.892	187.340	4.129
Skewness	0.596	0.784	0.864	-0.365	-0.213
Kurtosis	-0.681	-0.659	-0.458	-0.741	-1.145
Range	0.60	3.05	3.27	60.70	7.40
Minimum	0.10	0.45	0.57	5.80	3.80
Maximum	0.70	3.50	3.84	66.50	11.20

Table 2. Pearson correlation matrix of input and output variables

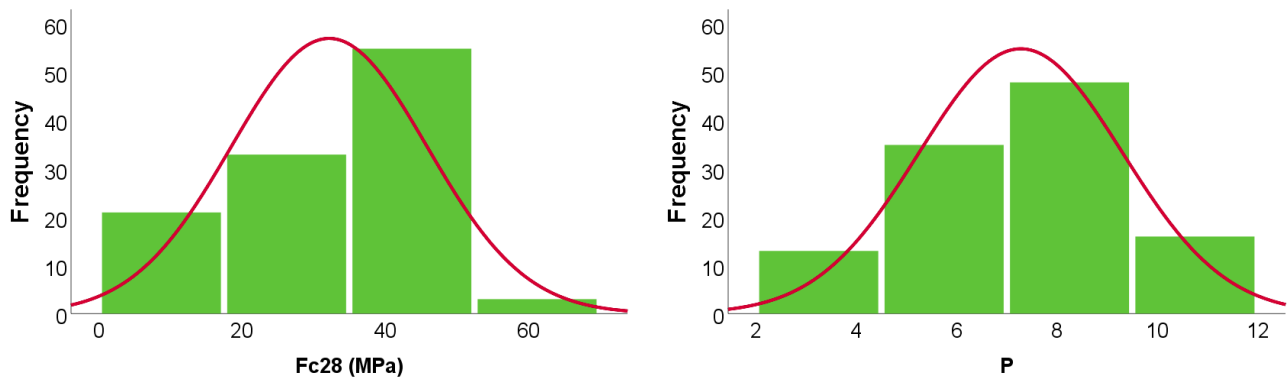|	FA/B	FAg/B	CAg/B	Fc28	P
FA/B	1.00				
FAg/B	0.30	1.00			
CAg/B	0.53	0.40	1.00		
Fc28	-0.55	-0.66	-0.59	1.00	
P	-0.46	-0.87	-0.72	0.68	1.00

Figure 2. Distribution histograms for inputs (in blue) and outputs (in green)

2.3. Research Modelling Plan

Three different models were used to predict the compressive strength and environmental impact factor of concrete mix using the gathered dataset. The implemented techniques are "traditional linear regression (TLR)" or "linear regression (LNR)", "artificial neural network (ANN)" and "evolutionary polynomial regression (EPR)" as presented in the last phase of the theoretical framework (Figure 1). All these techniques were used to predict 28 days compressive strength (Fc28, MPa) and the environmental impact factor (P) using only three parameters, fly Ash to binder ratio (FA/B), fine aggregates (Sand) to binder ratio (FAg/B) and coarse aggregates to binder ratio (CAg/B).

Each implemented technique is based on different approach mimicking human brain for ANN, optimization of mathematical regression for EPR and simulating evolution of natural creatures for GP. However, for all techniques, their accuracies were evaluated in terms of "sum of squared errors (SSE)", "root of mean of squared errors (RMSE)" and "determination coefficient (R^2)". The next sections present the results of each technique and its accuracy metrics.

3. Results and Analysis

3.1. General Remarks on Collected Concrete Mix Data and the Environmental Impact

Fly ash admixed concrete is characterized by its low greenhouses gas emission (GGE) potential, high workability potential, high reactivity, and reduced rheological behaviour but with high long-term strength development beyond 28 days curing period. However, the importance of utilizing little or no chemical cement like ordinary Portland cement (OPC) is emphasized in this research paper. In Figure 3 (also see Table 1), the compressive strength at 28 days curing and the environmental impact index (P) behaviour of FA admixed concrete corresponding to fly ash and binder ratio (FA/B; B = C+FA), fine aggregate and binder ratio (FAg/B) and coarse aggregate and binder ratio (CAg/B) is presented (see Figures 3-a to 3-f, respectively). It can be observed that the concrete mixes with high amount of cement produce high strength but with a compromised environment with high environmental impact (P) compared with the mixes with high FA and reduced cement, which produce low concrete strength (Fc28) but a more eco-friendly and eco-efficient environment with low impact (P) from the production and utilization of the concrete, which agrees with the studies [28-32, 41-53], which studied the sorbent effect of increased FA in concrete. By implication, this shows that high FA/B ratio produce low strength compared to low FA/B as presented in Figures 3-a and 3-b. This further means that high FA/B ratio implies that the FA amount is high compared to the amount of cement while low FA/B implies that the amount of FA has been compromised over the amount of cement.

Similarly, low FAg/B ratio produces high strength of concrete compared to high FAg/B ratio which produces relatively low concrete strength as presented in Figures 3-c and 3-d. This implies that while FAg amount is maintained, cement amount is required to be reduced more than the amount of FA in order to achieve improved strength of FA-based concrete for a healthier environment. In the case of CAg/B ratio as presented in Figures 3-e and 3-f, the effect of CAg amount is not actually of remarkable influence as research results have shown the less influence of CAg/B ratio over concrete strength and impact on the environment. It is important to note from examples taken from Figure 3 and Table 1 that the mix with the least amount of environmental impact of 3.8 produced a concrete strength as low as 9.6MPa with CAg/B ratio of 3.75, FAg/B ratio of 2.72 and FA/B ratio of 0.34. Conversely, the concrete mix with the highest compressive strength of 50.5MPa produced an impact point (P) of 7.4 with mix proportions of CAg/B ratio of 2.08, FAg/B ratio of 0.84 and FA/B ratio of 0.3. The emphasis of this exercise is on the FA/B ratio at almost the same value but produced strength difference of 40.9MPa (81% difference index). Greater percentage of the concrete mixes with considerably high amount of FA produce concrete with over 20.7MPa, which is the minimum required according to design standard for traditional concrete walls and columns [54, 55]. A good number of the mixes with good impact (P) according to ISO 14067 standard [56] produced strength (Fc28) above 27.6MPa, which is the minimum required for concrete pavements and a good number has strengths above 34.5MPa, which is the minimum required for concrete

structures in colder climate to withstand freeze and thaw cycles [54, 55]. Since a reduction in FA/B produces increased concrete strength, which implies either a reduction in FA amount or an increase in cement amount, the proposed models will become the tools to be deployed to maximize FA and minimize cement amount as to achieve optimal strength and minimal environmental impact.
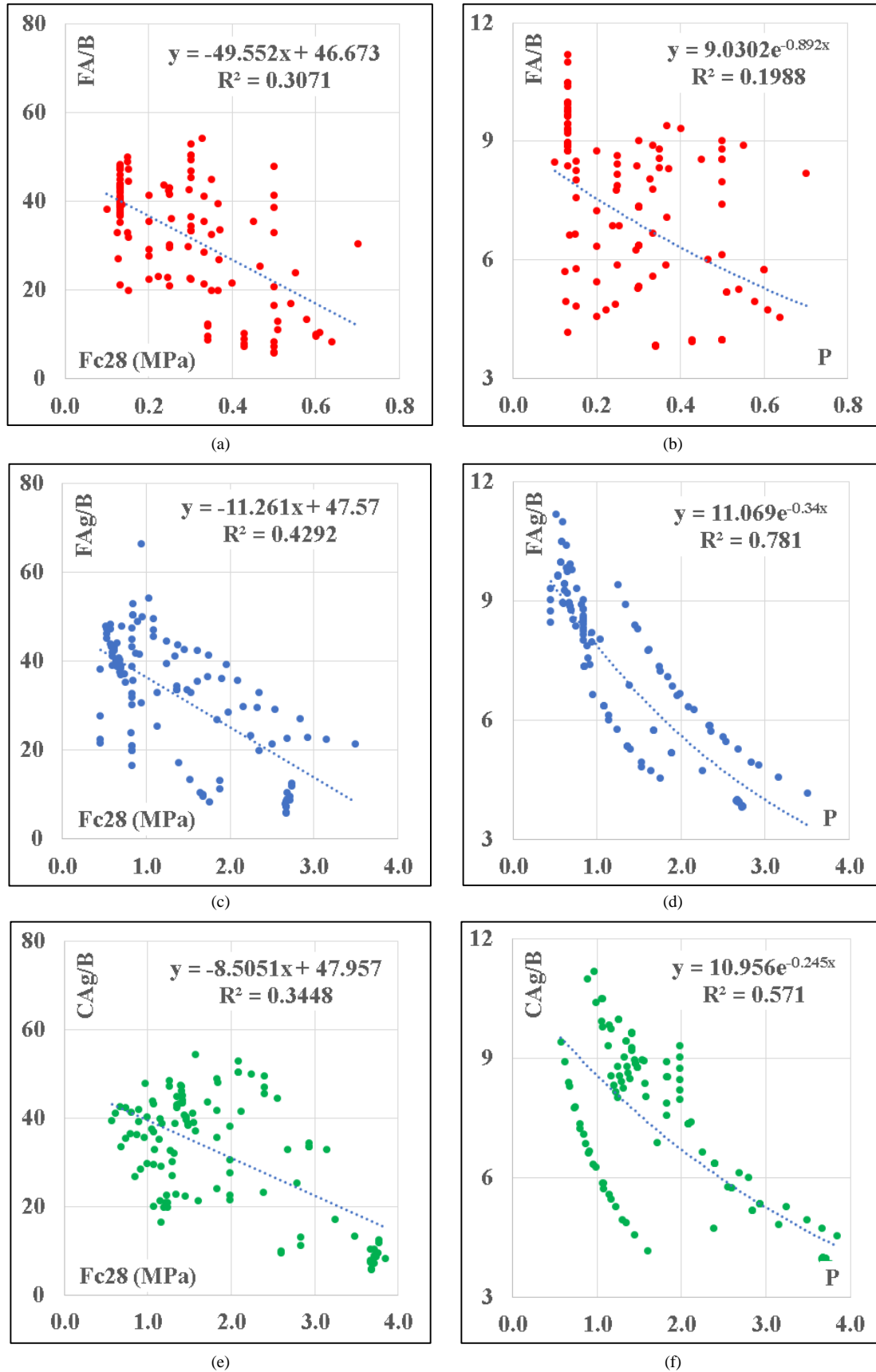

Figure 3. Compressive strength at 28 days (Fc28) and environmental impact point (P) behavior with respect to mix ratios of FA admixed concrete

3.2. Prediction of Compressive Strength and Environmental Impact of FA Admixed Concrete

3.2.1. Model (1) – Using TLR or LNR Technique

Linear regression (LNR) is a parallel approach for modeling the relationship between scalar responses and explanatory parameters, which are also known as dependent variables. It is a baseline regression technique employed as reference models in statistical analysis. This traditional technique, traditional linear regression (TLR), was used as a reference to evaluate the performance of the other (AI) techniques in the present research exercise, where FA/B, FAg/B, and CAg/B ratios are the independent (input) variables in a fly ash-admixed concrete mix production. Equations 1 and 2 present the output linear formulas for Fc28 and P, respectively, while Figures 8-a and 8-b show their fitness. The average error % of the total dataset is 26.5% and 7.9%, while the R^2 values are 0.481 and 0.912 in that order for Fc28 and P. This agrees with the performance of previous studies [57–60].

$$\text{Fc28} = 57.2 - 25\left(\frac{FA}{B}\right) - 8.1\left(\frac{FAg}{B}\right) - 3.58\left(\frac{CAg}{B}\right) \tag{1}$$

$$P = 11.47 - 0.31\left(\frac{FA}{B}\right) - 1.76\left(\frac{FAg}{B}\right) - 0.92\left(\frac{CAg}{B}\right) \tag{2}$$

3.2.2. Model (2) – Using ANN Technique

Two separate models were developed using ANN technique, one with layout of 3:6:1 to predict Fc28 and the other with layout of 3:2:1 to predict P. All the models used the traditional "Back Propagation (BP)" training algorithm, standardization method (Var/SD) and activation function (Hyper Tan).

The used networks layout for Fc28 is illustrated in Figure 4 and the relative importance of input parameters for Fc28 is presented in Figure 5 while the weight matrixes of the model is shown in Table 3. The used networks layout for P is illustrated in Figure 6 and the relative importance of input parameters for P is presented in Figure 7 while the weight matrixes of the model is shown in Table 4. The average errors in % of total dataset are 9.4% and 2.6% and the R^2 values are 0.955 and 0.991 for Fc28 and P, respectively. This agrees with a previous study [57] in terms of performance. The relative importance values for each input parameter for Fc28 and P indicates that Fc28 is almost equally affected by all inputs while P is mostly affected by the both aggregate percentages. The relations between calculated and predicted values are shown in Figure 8-c and Figure 8-d.

Figure 4. Architecture layout for the developed ANN for Fc28
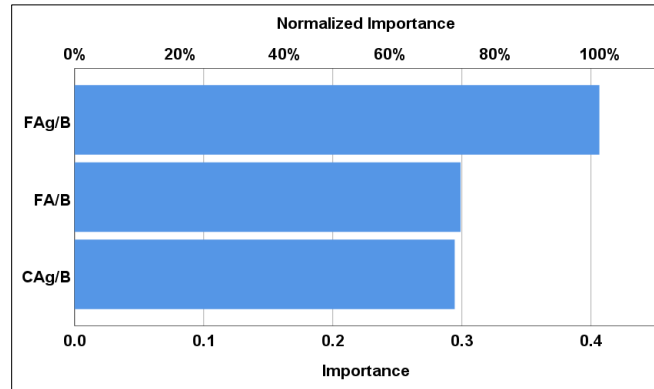
Figure 5. Relative importance of input parameters for Fc28

Table 3. Weights matrix for the developed ANN for Fc28

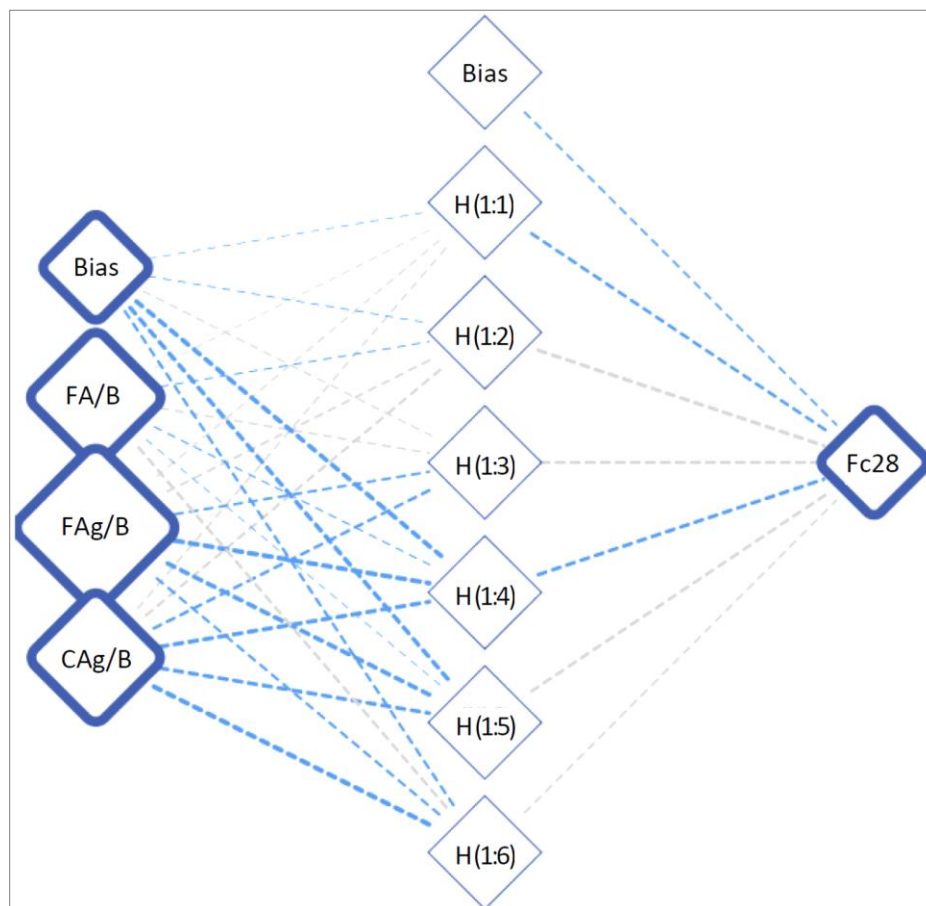|		Hidden Layer						
		H(1:1)	H(1:2)	H(1:3)	H(1:4)	H(1:5)	H(1:6)	
Input Layer	(Bias)	-0.05	-0.13	0.32	-12.18	-10.51	-1.83	
	FA/B	0.18	-0.19	0.35	-0.22	-0.07	3.46	
	FAg/B	0.30	0.79	-1.11	-12.91	-11.33	-1.24	
	CAg/B	0.34	1.84	-2.20	-5.91	-4.80	-15.62	
		Hidden Layer						
		H(1:1)	H(1:2)	H(1:3)	H(1:4)	H(1:5)	H(1:6)	(Bias)
Fc28		-2.70	5.84	4.32	-3.84	3.52	0.59	-0.43
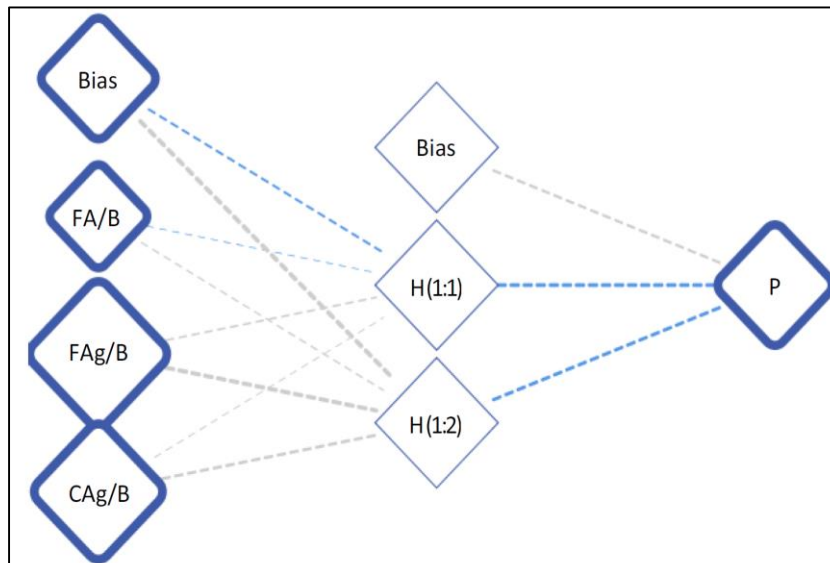
Figure 6. Architecture layout for the developed ANN for P
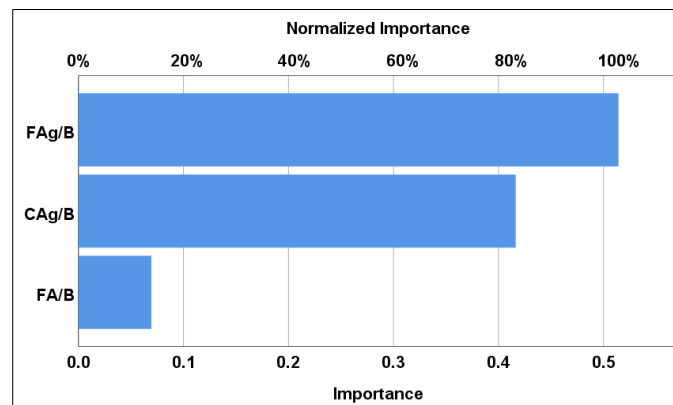
Figure 7. Relative importance of input parameters for P

Table 4. Weights matrix for the developed ANN for P

		Hidden Layer	
		H(1:1)	**H(1:2)**
Input Layer	(Bias)	-0.25	4.91
	FA/B	-0.03	0.18
	FAg/B	0.18	2.97
	CAg/B	0.15	1.22

	Hidden Layer		
	H(1:1)	**H(1:2)**	**(Bias)**
P	-2.66	-2.01	1.14
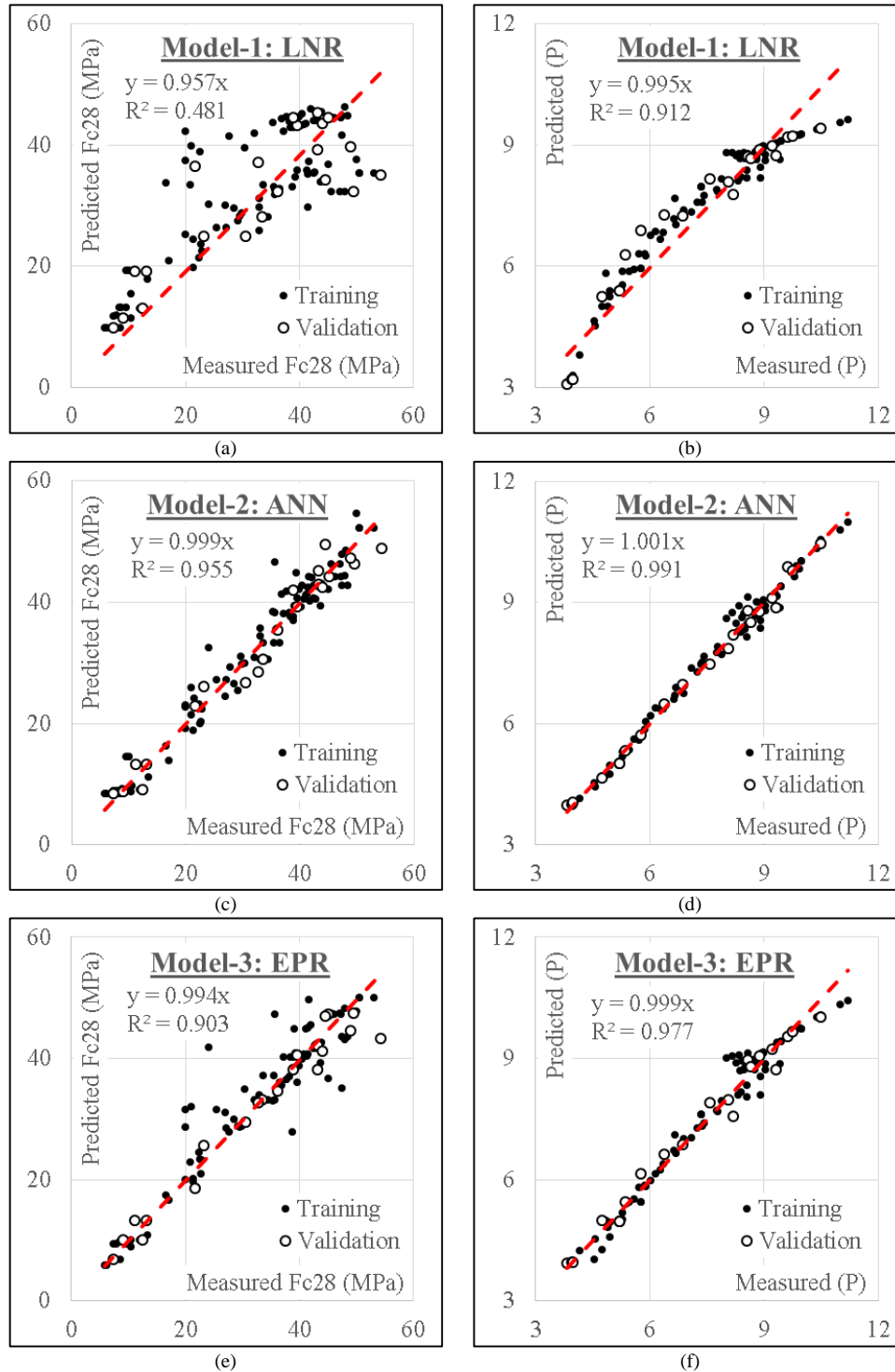
Figure 8. Relation between predicted and calculated values; a) LNR Fc28, b) LNR P, c) ANN Fc28, d) ANN P, e) EPR Fc28 and f) EPR P using the developed models

3.2.3 Model (3) – Using EPR Technique

Finally, the developed EPR model was limited to quadrilateral level for (Fc28) and quadratic level for (P), for three inputs, there are 35 possible terms (15+10+6+3+1=35) for (Fc28) and only (10) teams for (P) as follows:

$$\sum_{i=1}^{i=3}\sum_{j=1}^{j=3}\sum_{k=1}^{k=3}\sum_{l=1}^{l=3} X_i \cdot X_j \cdot X_k \cdot X_l + \sum_{i=1}^{i=3}\sum_{j=1}^{j=3}\sum_{k=1}^{k=3} X_i \cdot X_j \cdot X_k + \sum_{i=1}^{i=3}\sum_{j=1}^{j=3} X_i \cdot X_j + \sum_{i=1}^{i=3} X_i + C \tag{3}$$

The GA technique was applied to this polynomial to select the most effective 28 terms to predict Fc28 and 5 teams to predict P. The outputs are illustrated in Equations 4 and 5, and their fitness is shown in Figures 8-e and 8-f. The average error% and R^2 values are 13.9% and 0.903 and 4.2% and 0.977 for Fc28 and P, respectively. The results of all developed models are summarized in Table 5. Generally, Figures 9 and 10 show the Taylor's and variance diagrams, which illustrate the behavior of the models for Fc28 and P compared to the measured values. In Figure 9-a, it can be observed that the ANN and EPR models for Fc28 lie within the RMSE envelop of less than 0.5% and the standard deviation of between 15 MPa and 20 MPa, while the coefficient of determination sector lies between 95% and 99% except for LNR, which lies in the region of less than 80%. This agrees with a previous study [57] in terms of performance. In the case of the P models, all the predicted models lie within the RMSE envelop of between 0.5% and 1.0%, a coefficient of determination sector of 95% and above, and a standard deviation between 2.0 and 3.0 points of impact. This performance agrees with the previous performance published in literature [58–61]. In Figure 10, the variance between measured and modeled values is illustrated. It can be observed that ANN has the best distribution variance in Figures 10a and 10b for Fc28 and P models, respectively, which agrees with the performance accuracy and fits presented in Figure 8 and Table 5.

$$\text{Fc28} = \left(\frac{FA}{B}\right)^2\left[61.6\left(\frac{CAg}{B}\right) - 157\left(\frac{FAg}{B}\right) - 52.2\left(\frac{B}{FAg}\right) - 10.3\left(\frac{B}{CAg}\right) - 26.3\right] + \left(\frac{CAg}{B}\right)^2\left[45.8\left(\frac{FA}{B}\right) + \right.$$
$$15.7\left(\frac{FAg}{B}\right) - 14.6\left(\frac{B}{FAg}\right) - 57.8\right] + \left(\frac{FAg}{B}\right)^2\left[13.6 - 1.15\left(\frac{B}{FA}\right)\right] + \left(\frac{FA}{B}\right)\left(\frac{B}{FAg}\right)\left[357 - 77.6\left(\frac{CAg}{B}\right) - \right.$$
$$\left.428\left(\frac{B}{CAg}\right)\right] + \left(\frac{B}{FA}\right)\left(\frac{B}{FAg}\right)\left[21.6 - 7.0\left(\frac{CAg}{B}\right) - 6.8\left(\frac{B}{CAg}\right)\right] + \left(\frac{B}{FA}\right)\left(\frac{FAg}{B}\right)\left[25.6 - 8.0\left(\frac{CAg}{B}\right) - \right.$$
$$\left.9.6\left(\frac{B}{CAg}\right)\right] + \left(\frac{CAg}{B}\right)\left[25.5\left(\frac{B}{FA}\right) - 149\left(\frac{FA}{B}\right) - 72.3\left(\frac{FAg}{B}\right) + 293\right] + \left(\frac{B}{FA}\right)\left[45.0\left(\frac{B}{CAg}\right) - 82.6\right] +$$
$$358\left(\frac{FA}{B}\right)\left(\frac{B}{CAg}\right) - 178 \tag{4}$$

$$P = 14.2 - 4.1\left(\frac{FAg}{B}\right) + 0.62\left(\frac{FAg}{B}\right)\left(\frac{CAg}{B}\right) + 0.35\left(\frac{FAg}{B}\right)^2 - 2.15\left(\frac{GAg}{B}\right) \tag{5}$$

(a)   (b)
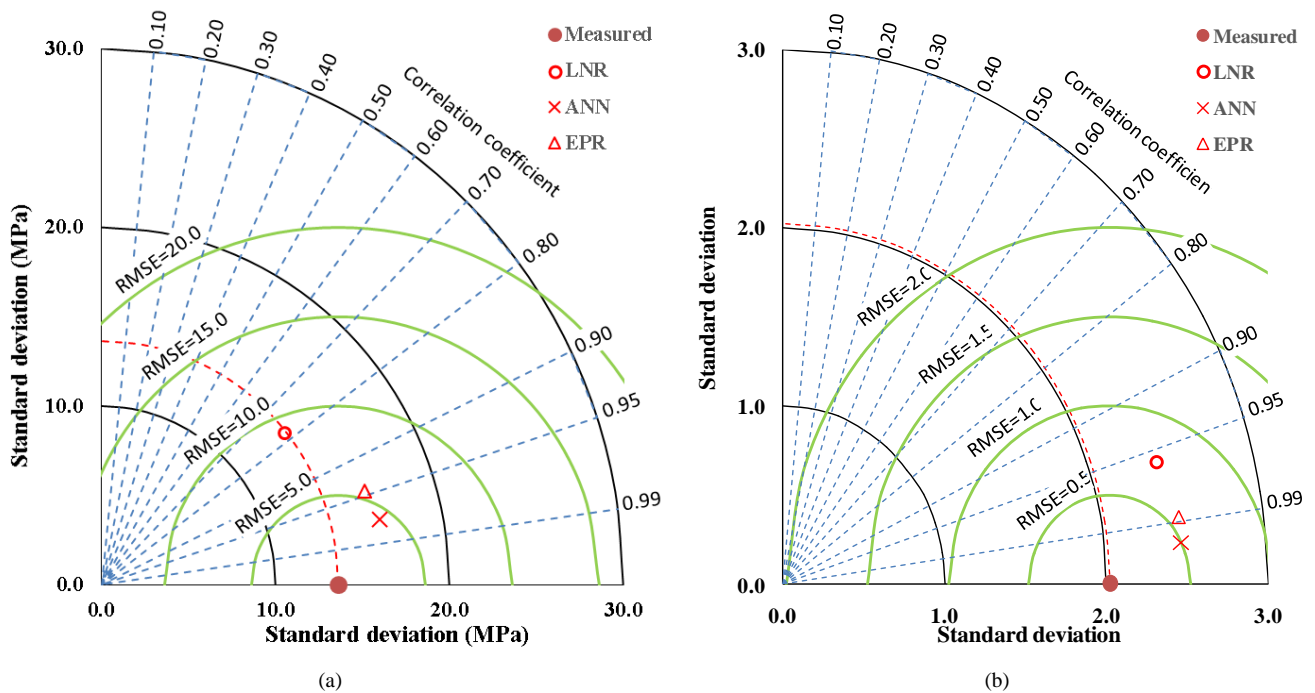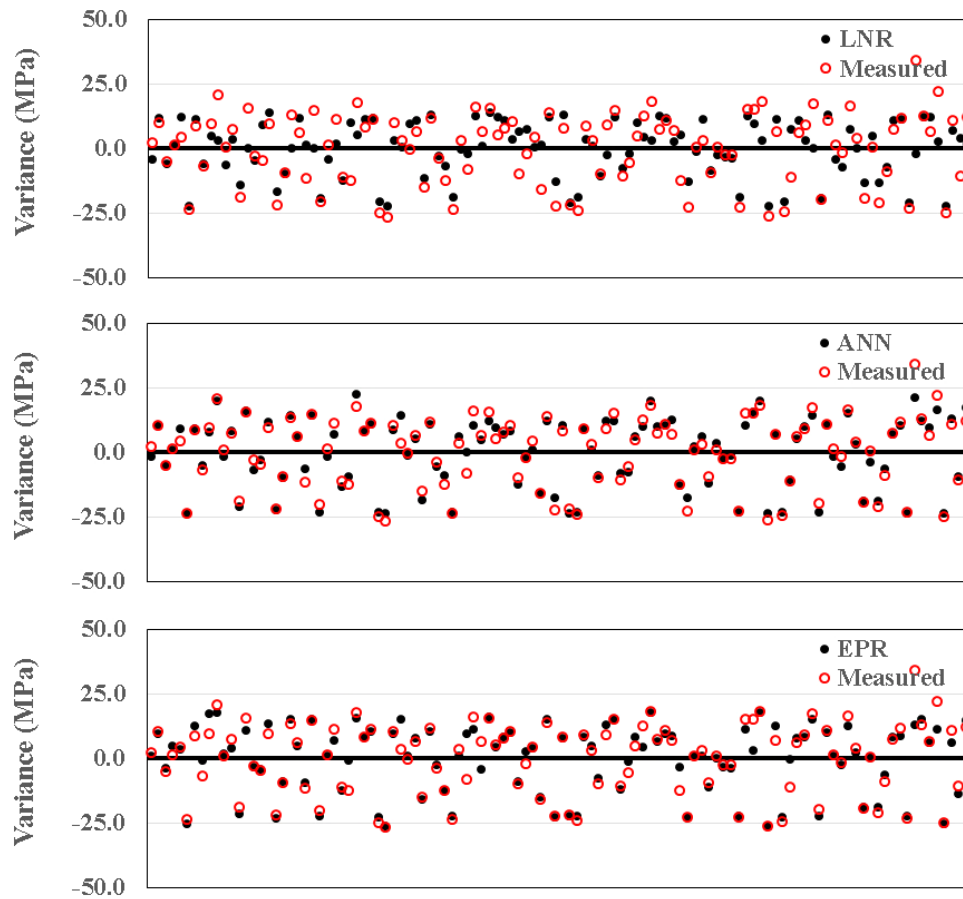
Figure 9. Comparison between developed models; a) Fc28 and b) P using Taylor diagram

(a) Fc28
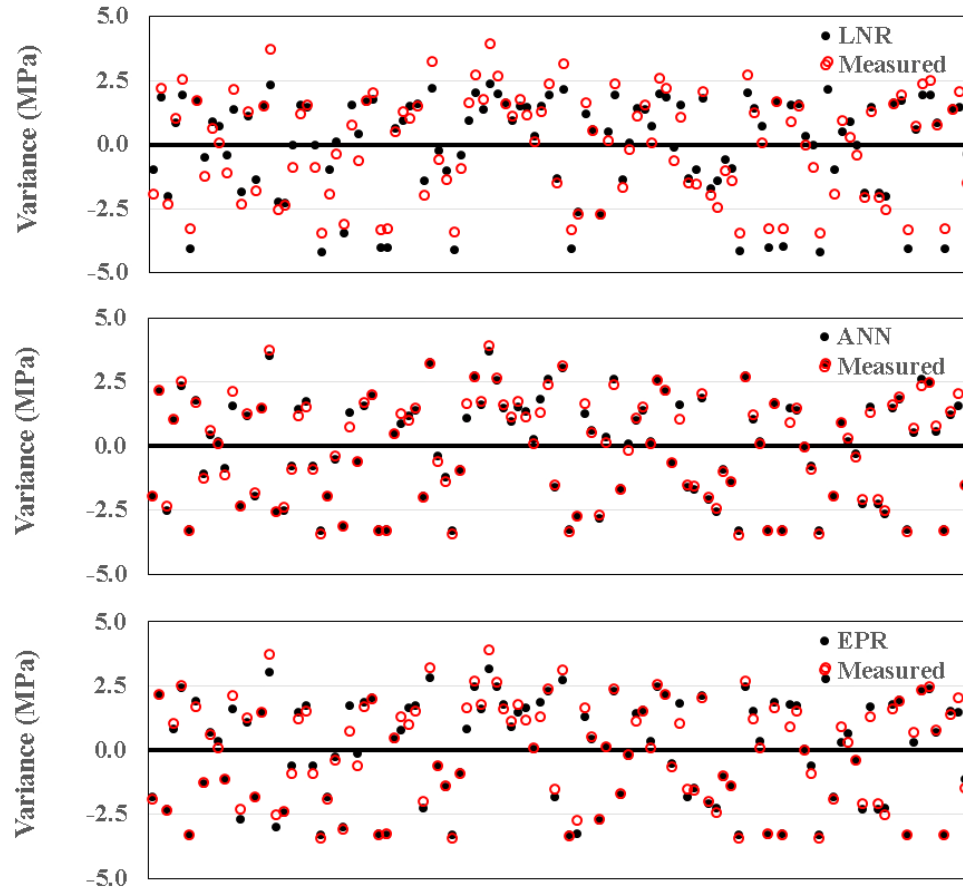
(b) P

Figure 10. Comparison between developed models; a) Fc28 and b) P using Variance diagrams

Table 5. Performance accuracies of developed models

Item	Technique	Model	SSE	Avg. Error %	R^2
	LNR	Eq. 1	8141	26.5	0.481
Fc28	ANN	Fig. 2, Table 3	1023	9.4	0.955
	EPR	Eq. 3	2234	13.9	0.903
	LNR	Eq. 2	37	7.9	0.912
P	ANN	Fig. 4, Table 4	4	2.6	0.991
	EPR	Eq.4	11	4.2	0.977

3.3. The ANN Developed Mix Design Aid

Although the predictive models developed for Fc28 using ANN and EPR are accurate enough, but they are still hard to implement in practical mix designs especially for manual calculations. Hence, a concrete mix design tool was developed by substituting in the developed ANN model with different combinations of input parameters values varied with constant intervals. Then the calculated Fc28 values, while Figure 11 presents the corresponding binder content (B) and water-binder ratio (W/B) for each input parameter combination, were plotted on the contour charts shown in Figure 12. The key chart indicates the changes in mix design when moving toward each corner of the design chart, where moving on the diagonal (top left – bottom right) changes the fine-coarse aggregate ratio with constant binder content and water-binder ratio, while moving along the other diagonal inversely changes the binder content and water-binder ratio. Using this mix design tool is very simple with only the desired (Fc28) and fly ash-binder ratio (FA/B) taken into knowledge. Just select the correct chart in Figure 12 based on FA/B value, then locate the required Fc28 on the selected chart to determine both (FAg/B) and (CAg/B). From the corresponding cells in Figure 11, both binder content (B) (ton/m³) and water-binder ratio (W/B) could be determined. Finally, the absolute values of water, fly ash, fine and coarse aggregates could be calculated by multiplying their ratios by the binder content.

Figure 11. Concrete mix design aid, key chat, corresponding binder content (B) and water-binder ratio (W/B) for diffident combinations of (FA/B), (Fag/B) & (Cag/B)

CAg/B

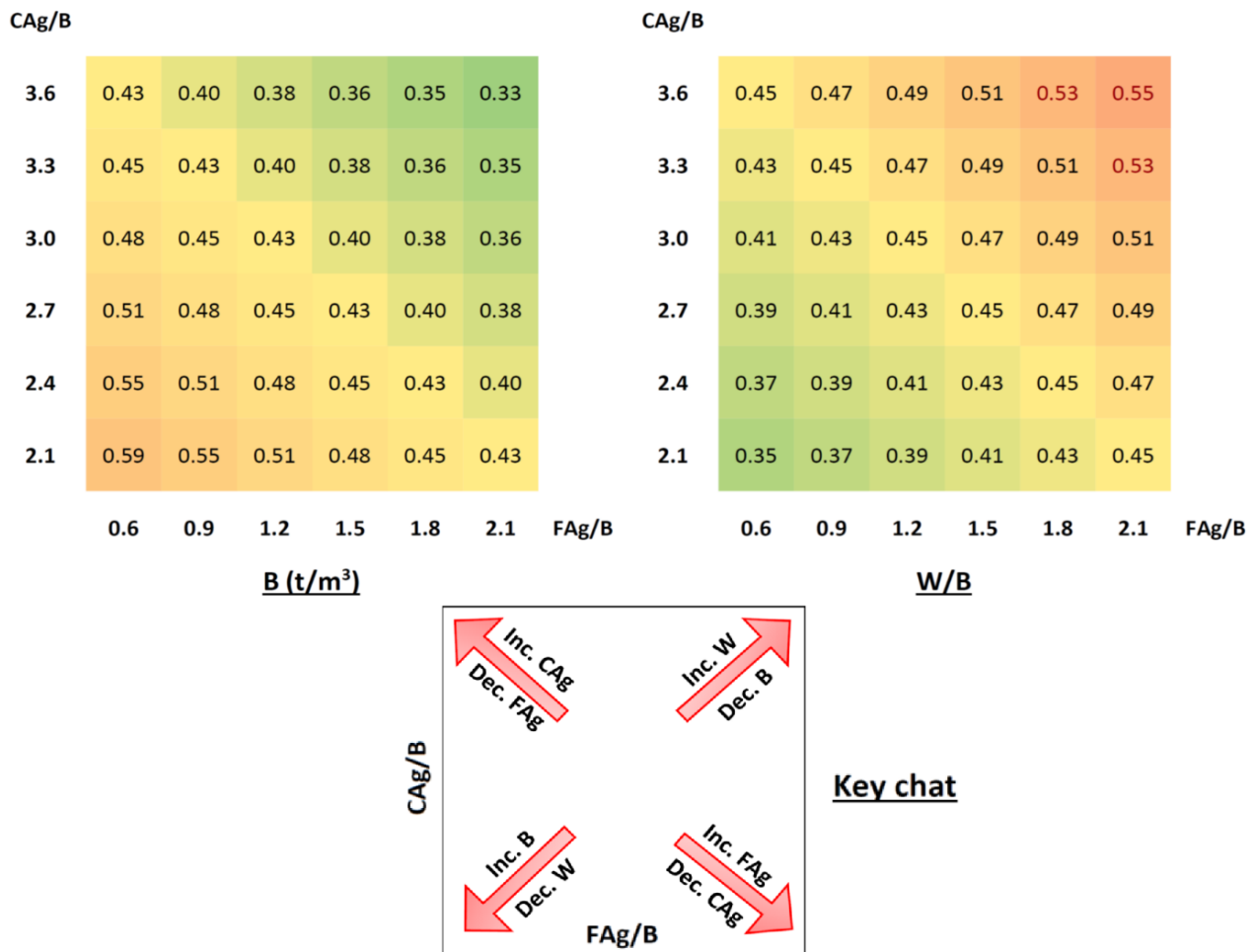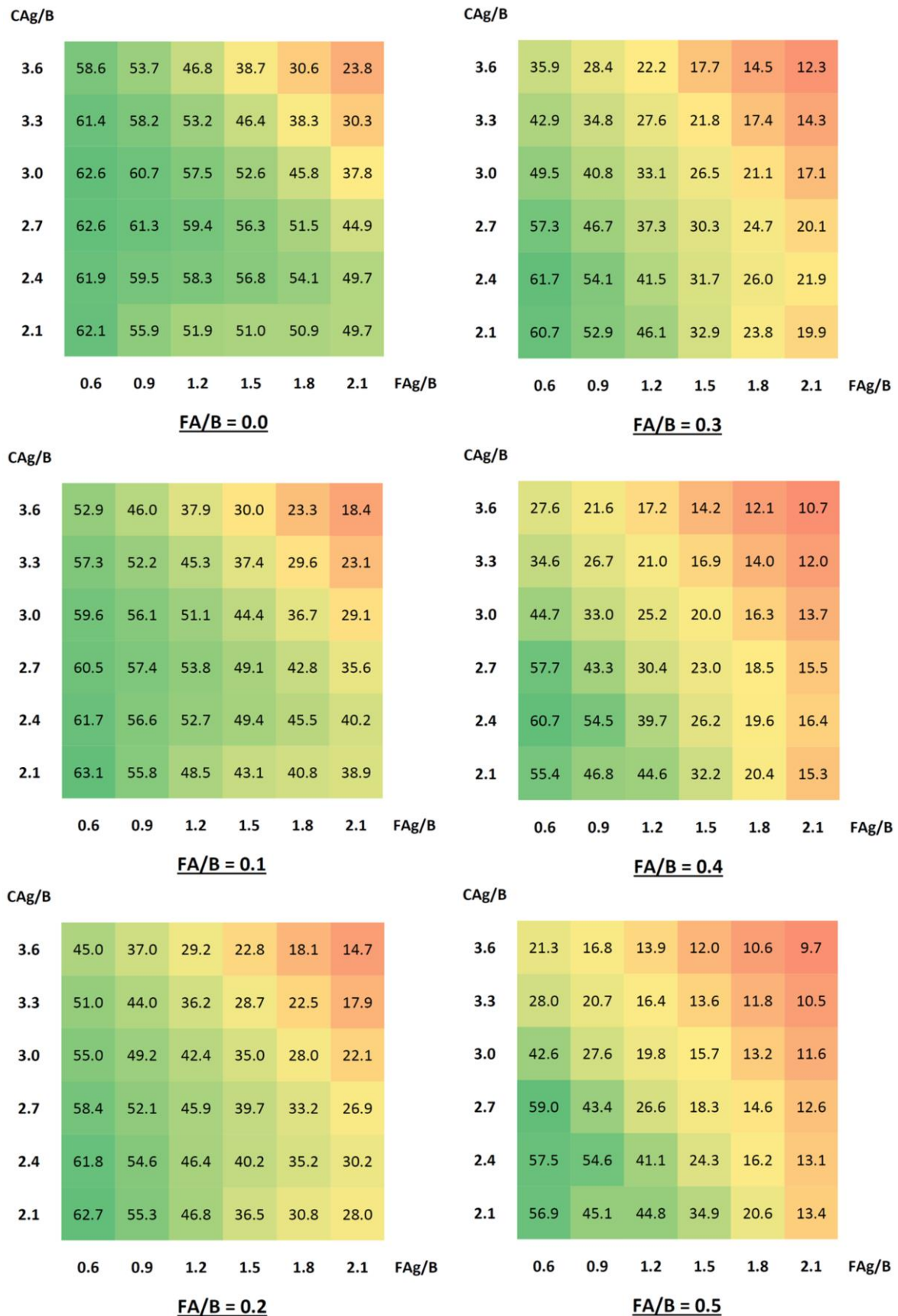| 3.6 | 58.6 | 53.7 | 46.8 | 38.7 | 30.6 | 23.8 |
3.3	61.4	58.2	53.2	46.4	38.3	30.3
3.0	62.6	60.7	57.5	52.6	45.8	37.8
2.7	62.6	61.3	59.4	56.3	51.5	44.9
2.4	61.9	59.5	58.3	56.8	54.1	49.7
2.1	62.1	55.9	51.9	51.0	50.9	49.7
	0.6	0.9	1.2	1.5	1.8	2.1	FAg/B

FA/B = 0.0

CAg/B

3.6	35.9	28.4	22.2	17.7	14.5	12.3
3.3	42.9	34.8	27.6	21.8	17.4	14.3
3.0	49.5	40.8	33.1	26.5	21.1	17.1
2.7	57.3	46.7	37.3	30.3	24.7	20.1
2.4	61.7	54.1	41.5	31.7	26.0	21.9
2.1	60.7	52.9	46.1	32.9	23.8	19.9
	0.6	0.9	1.2	1.5	1.8	2.1	FAg/B

FA/B = 0.3

CAg/B

3.6	52.9	46.0	37.9	30.0	23.3	18.4
3.3	57.3	52.2	45.3	37.4	29.6	23.1
3.0	59.6	56.1	51.1	44.4	36.7	29.1
2.7	60.5	57.4	53.8	49.1	42.8	35.6
2.4	61.7	56.6	52.7	49.4	45.5	40.2
2.1	63.1	55.8	48.5	43.1	40.8	38.9
	0.6	0.9	1.2	1.5	1.8	2.1	FAg/B

FA/B = 0.1

CAg/B

3.6	27.6	21.6	17.2	14.2	12.1	10.7
3.3	34.6	26.7	21.0	16.9	14.0	12.0
3.0	44.7	33.0	25.2	20.0	16.3	13.7
2.7	57.7	43.3	30.4	23.0	18.5	15.5
2.4	60.7	54.5	39.7	26.2	19.6	16.4
2.1	55.4	46.8	44.6	32.2	20.4	15.3
	0.6	0.9	1.2	1.5	1.8	2.1	FAg/B

FA/B = 0.4

CAg/B

3.6	45.0	37.0	29.2	22.8	18.1	14.7
3.3	51.0	44.0	36.2	28.7	22.5	17.9
3.0	55.0	49.2	42.4	35.0	28.0	22.1
2.7	58.4	52.1	45.9	39.7	33.2	26.9
2.4	61.8	54.6	46.4	40.2	35.2	30.2
2.1	62.7	55.3	46.8	36.5	30.8	28.0
	0.6	0.9	1.2	1.5	1.8	2.1	FAg/B

FA/B = 0.2

CAg/B

3.6	21.3	16.8	13.9	12.0	10.6	9.7
3.3	28.0	20.7	16.4	13.6	11.8	10.5
3.0	42.6	27.6	19.8	15.7	13.2	11.6
2.7	59.0	43.4	26.6	18.3	14.6	12.6
2.4	57.5	54.6	41.1	24.3	16.2	13.1
2.1	56.9	45.1	44.8	34.9	20.6	13.4
	0.6	0.9	1.2	1.5	1.8	2.1	FAg/B

FA/B = 0.5

Figure 12. Concrete mix design aid, (Fc28) for diffident combinations of (FA/B), (Fag/B) and (Cag/B)

For example, to design a concrete mix with Fc28 = 40 MPa and FA/B = 20%, the lower left chart in Figure 12 will be used, (FAg/B) is 1.5 and (CAg/B) lies between 2.4 and 2.7 (almost 2.55 by interpolation). From Figure 11, the binder content lays between 0.43 and 0.45 t/m3 (almost 0.44 t/m3 by interpolation) and (W/B) lays also between 43% and 45% (almost 0.44 % by interpolation principle). Hence, 1.0 m3 of this mix contains 350 kg of cement (C), 90 kg of fly ash

(FA), 194 liters of water (W), 660 kg of fine aggregate (sand) (FAg), and 1125 kg of coarse aggregate (CAg). On the environmental impact considerations with respect to the mix design tool, there exists a straight-line relationship between the concrete strength at 28 days (Fc28) and the fly ash content (FA). This shows that in considering the optimization of strength (maximal value) and environmental impact index at minimal value, there must be an optimized value of FA required at any point to achieve optimal Fc with the corresponding W/B, FAg, and CAg values. With this achieved, a concrete mix with less or no negative impact from greenhouse gas emissions is designed for more sustainable and greener infrastructure.

4. Conclusions

This research presents three models using three techniques (LNR, ANN, and EPR) to predict both the 28-day compressive strength (Fc28) and the environmental impact factor (P) using only three parameters: fly ash to binder ratio (FA/B), fine aggregates (sand) to binder ratio (Fag/B), and coarse aggregates to binder ratio (Cag/B). Also, the research presented a concrete mix design tool developed based on the ANN predictive model.

The results of comparing the accuracies of the developed models could be concluded in the following points:

- The traditional linear regression technique was used as a reference to evaluate the performance of the other models. It showed the worst accuracy for both Fc28 and P of 73.5% and 92.1%, respectively.

- (ANN) models showed the best accuracy of 91.6% and 97.4% for Fc28 and P, respectively. In spite of its high accuracy, it is still too difficult to implement manually. The newly developed mix design tool provides a quick and easy alternative to the long and complicated calculations of ANN.

- Finally, the EPR model presents a less complicated and also less accurate alternative to the ANN, where its accuracies are 86.1% and 95.8% for both Fc28 and P, respectively.

- The summation of the absolute weights of each neuron in the input layer of the developed ANN model indicates that Fc28 is almost equally affected by all input values, while P is mainly affected by aggregate-binder ratios. This conclusion is confirmed by EPR models, where the formula P includes only aggregate ratios.

- The EPR-GA technique successfully reduced the 35 and 10 terms of the conventional polynomial regression quadrilateral formula to only 28 and 5 terms for Fc28 and P, respectively, without having a significant impact on its accuracy.

- Like any other regression technique, the generated formulas are valid within the considered range of parameter values; beyond this range, the prediction accuracy should be verified.

- Like any other regression technique, the generated formulas are valid within the considered range of parameter values; beyond this range, the prediction accuracy should be verified:

- This tool (charts) is limited to the following ranges:

  o Binder content, 330 to 590 kg/m^3

  o Water-binder ratio, 35% to 55%

  o Fly ash – binder ratio, 0.0% to 50%

  o Fine aggregate – binder ratio, 0.6 to 2.1

  o Coarse aggregate – binder ratio, 2.1 to 3.6

  o Fc28, 10 to 63 MPa

- Generally, increasing the fly ash-binder ratio decreases the Fc28.

- Decreasing both of the aggregate-binder ratios together increases the Fc28 due to increasing the binder content and reduces the water-binder ratio, and vice versa (moving along the top right – bottom left diagonal).

- Increasing the coarse aggregate ratio and decreasing the fine aggregate ratio with constant binder content and water-binder ratio increases the Fc28 value (moving along the bottom right-top left diagonal).

Further studies may be carried out to predict other properties of fresh and hardened concrete, such as workability, tensile strength, and elastic modulus.

5. Declarations

5.1. Author Contributions

5.2. Data Availability Statement

The data presented in this study are openly available in the appendix I.

5.3. Funding

5.4. Conflicts of Interest

The authors declare no conflict of interest.

6. References

[1] Amran, M., Fediuk, R., Murali, G., Avudaiappan, S., Ozbakkaloglu, T., Vatin, N., Karelina, M., Klyuev, S., & Gholampour, A. (2021). Fly ash-based eco-efficient concretes: A comprehensive review of the short-term properties. Materials, 14(15), 4264. doi:10.3390/ma14154264.

[2] Lakshmi, R., & Nagan, S. (2011). Utilization of waste e plastic particles in cementitious mixtures. Journal of Structural Engneering (Madras), 38(1), 26–35.

[3] Malhotra, V. High-performance high-volume fly ash concrete. Concrete International, 24(7), 30–34.

[4] Castel, A., & Foster, S. J. (2015). Bond strength between blended slag and Class F fly ash geopolymer concrete with steel reinforcement. Cement and Concrete Research, 72, 48–53. doi:10.1016/j.cemconres.2015.02.016.

[5] Hossain, M. U., Poon, C. S., Dong, Y. H., & Xuan, D. (2018). Evaluation of environmental impact distribution methods for supplementary cementitious materials. Renewable and Sustainable Energy Reviews, 82, 597–608. doi:10.1016/j.rser.2017.09.048.

[6] Li, Y., Liu, Y., Gong, X., Nie, Z., Cui, S., Wang, Z., & Chen, W. (2016). Environmental impact analysis of blast furnace slag applied to ordinary Portland cement production. Journal of Cleaner Production, 120, 221–230. doi:10.1016/j.jclepro.2015.12.071.

[7] Abdalqader, A. F., Jin, F., & Al-Tabbaa, A. (2016). Development of greener alkali-activated cement: Utilisation of sodium carbonate for activating slag and fly ash mixtures. Journal of Cleaner Production, 113, 66–75. doi:10.1016/j.jclepro.2015.12.010.

[8] Krishnan, S., Emmanuel, A.C., Bishnoi, S. (2015). Effective Clinker Replacement Using SCM in Low Clinker Cements. Calcined Clays for Sustainable Concrete. RILEM Bookseries, 10, Springer, Dordrecht, Netherlands. doi:10.1007/978-94-017-9939-3_64.

[9] Guynn, J., & Kline, J. (2015). Maximizing SCM Content of Blended Cements. IEEE Transactions on Industry Applications, 51(6), 4824–4832. doi:10.1109/TIA.2015.2455029.

[10] Flower, D. J. M., & Sanjayan, J. G. (2017). Greenhouse Gas Emissions Due to Concrete Manufacture. Handbook of Low Carbon Concrete, 1–16, Butterworth-Heinemann, Oxford, United Kingdom. doi:10.1016/b978-0-12-804524-4.00001-4.

[11] Habert, G., D'Espinose De Lacaillerie, J. B., & Roussel, N. (2011). An environmental evaluation of geopolymer based concrete production: Reviewing current research trends. Journal of Cleaner Production, 19(11), 1229–1238. doi:10.1016/j.jclepro.2011.03.012.

[12] De Schepper, M., Van den Heede, P., Van Driessche, I., & De Belie, N. (2014). Life Cycle Assessment of Completely Recyclable Concrete. Materials, 7(8), 6010–6027. doi:10.3390/ma7086010.

[13] González-Fonteboa, B., & Martínez-Abella, F. (2008). Concretes with aggregates from demolition waste and silica fume. Materials and mechanical properties. Building and Environment, 43(4), 429–437. doi:10.1016/j.buildenv.2007.01.008.

[14] Zhang, J., Cheng, J. C. P., & Lo, I. M. C. (2014). Life cycle carbon footprint measurement of Portland cement and ready mix concrete for a city with local scarcity of resources like Hong Kong. International Journal of Life Cycle Assessment, 19(4), 745–757. doi:10.1007/s11367-013-0689-7.

[15] Safiuddin, M., Raman, S. N., & Muhammad, M. F. (2015). Effects of medium temperature and industrial by-products on the key hardened properties of high performance concrete. Materials, 8(12), 8608–8623. doi:10.3390/ma8125464.

[16] Pacheco Torgal, F., Miraldo, S., Labrincha, J. A., & De Brito, J. (2012). An overview on concrete carbonation in the context of eco-efficient construction: Evaluation, use of SCMs and/or RAC. Construction and Building Materials, 36, 141–150. doi:10.1016/j.conbuildmat.2012.04.066.

[17] Teixeira, E. R., Mateus, R., Camões, A. F., Bragança, L., & Branco, F. G. (2016). Comparative environmental life-cycle analysis of concretes using biomass and coal fly ashes as partial cement replacement material. Journal of Cleaner Production, 112, 2221–2230. doi:10.1016/j.jclepro.2015.09.124.

[18] Kou, S. C., & Poon, C. S. (2013). A novel polymer concrete made with recycled glass aggregates, fly ash and metakaolin. Construction and Building Materials, 41, 146–151. doi:10.1016/j.conbuildmat.2012.11.083.

[19] Poon, C. S., & Chan, D. (2006). Paving blocks made with recycled concrete aggregate and crushed clay brick. Construction and Building Materials, 20(8), 569–577. doi:10.1016/j.conbuildmat.2005.01.044.

[20] Amran, Y. H. M., Alyousef, R., Alabduljabbar, H., & El-Zeadani, M. (2020). Clean production and properties of geopolymer concrete; A review. Journal of Cleaner Production, 251, 119679. doi:10.1016/j.jclepro.2019.119679.

[21] ASTM C618-22. (2022). Standard Specification for Coal Fly Ash and Raw or Calcined Natural Pozzolan for Use in Concrete. ASTM International, Pennsylvania, United States. doi:10.1520/C0618-22.

[22] Liu, J., Fan, X., Li, Z., Zhang, W., Jin, H., Xing, F., & Tang, L. (2022). Novel recycling application of high volume municipal solid waste incineration bottom ash (MSWIBA) into sustainable concrete. Science of the Total Environment, 838, 156124. doi:10.1016/j.scitotenv.2022.156124.

[23] Abdalla, A., & Salih, A. (2022). Microstructure and chemical characterizations with soft computing models to evaluate the influence of calcium oxide and silicon dioxide in the fly ash and cement kiln dust on the compressive strength of cement mortar. Resources, Conservation & Recycling Advances, 15, 200090. doi:10.1016/j.rcradv.2022.200090.

[24] ISO 14040:2006. (2006). Environmental management—life cycle assessment—principles and framework. International Organization for Standards (ISO), Geneva, Switzerland.

[25] Xu, G., & Shi, X. (2018). Characteristics and applications of fly ash as a sustainable construction material: A state-of-the-art review. Resources, Conservation and Recycling, 136, 95–109. doi:10.1016/j.resconrec.2018.04.010.

[26] Seto, K. E., Churchill, C. J., & Panesar, D. K. (2017). Influence of fly ash allocation approaches on the life cycle assessment of cement-based materials. Journal of Cleaner Production, 157, 65–75. doi:10.1016/j.jclepro.2017.04.093.

[27] Tosun-Felekoğlu, K., Gödek, E., Keskinateş, M., & Felekoğlu, B. (2017). Utilization and selection of proper fly ash in cost effective green HTPP-ECC design. Journal of Cleaner Production, 149, 557–568. doi:10.1016/j.jclepro.2017.02.117.

[28] Balaguera, A., Carvajal, G. I., Albertí, J., & Fullana-i-Palmer, P. (2018). Life cycle assessment of road construction alternative materials: A literature review. Resources, Conservation and Recycling, 132, 37–48. doi:10.1016/j.resconrec.2018.01.003.

[29] Poinot, T., Laracy, M. E., Aponte, C., Jennings, H. M., Ochsendorf, J. A., & Olivetti, E. A. (2018). Beneficial use of boiler ash in alkali-activated bricks. Resources, Conservation and Recycling, 128, 1–10. doi:10.1016/j.resconrec.2017.09.013.

[30] Huang, T. Y., Chiueh, P. T., & Lo, S. L. (2017). Life-cycle environmental and cost impacts of reusing fly ash. Resources, Conservation and Recycling, 123, 255–260. doi:10.1016/j.resconrec.2016.07.001.

[31] Wang, P., Wang, J., Qin, Q., & Wang, H. (2017). Life cycle assessment of magnetized fly-ash compound fertilizer production: A case study in China. Renewable and Sustainable Energy Reviews, 73, 706–713. doi:10.1016/j.rser.2017.02.005.

[32] Ahmaruzzaman, M., & Gupta, V. K. (2012). Application of coal fly ash in air quality management. Industrial and Engineering Chemistry Research, 51(47), 15299–15314. doi:10.1021/ie301336m.

[33] Siddique, R. (2011). Properties of self-compacting concrete containing class F fly ash. Materials and Design, 32(3), 1501–1507. doi:10.1016/j.matdes.2010.08.043.

[34] Jalal, M., Pouladkhan, A., Harandi, O. F., & Jafari, D. (2015). Comparative study on effects of Class F fly ash, nano silica and silica fume on properties of high performance self-compacting concrete. Construction and Building Materials, 94, 90–104. doi:10.1016/j.conbuildmat.2015.07.001.

[35] Matos, P. R. de, Foiato, M., & Prudêncio, L. R. (2019). Ecological, fresh state and long-term mechanical properties of high-volume fly ash high-performance self-compacting concrete. Construction and Building Materials, 203, 282–293. doi:10.1016/j.conbuildmat.2019.01.074.

[36] Jong, L. Y., & Teo, D. C. L. (2014). Concrete Containing Palm Oil Fuel Ash (POFA) and Oil Palm Shell (OPS) Subjected to Elevated Temperatures. Journal of Civil Engineering, Science and Technology, 5(3), 13–17. doi:10.33736/jcest.140.2014.

[37] Chernysheva, N., Lesovik, V., Fediuk, R., & Vatin, N. (2020). Improvement of performances of the gypsum-cement fiber reinforced composite (GCFRC). Materials, 13(17), 3847. doi:10.3390/ma13173847.

[38] Pala, M., Özbay, E., Öztaş, A., & Yuce, M. I. (2007). Appraisal of long-term effects of fly ash and silica fume on compressive strength of concrete by neural networks. Construction and Building Materials, 21(2), 384–394. doi:10.1016/j.conbuildmat.2005.08.009.

[39] Chopra, P., Sharma, R. K., & Kumar, M. (2016). Prediction of Compressive Strength of Concrete Using Artificial Neural Network and Genetic Programming. Advances in Materials Science and Engineering, 2016, 1–10. doi:10.1155/2016/7648467.

[40] Yuan, Z., Wang, L. N., & Ji, X. (2014). Prediction of concrete compressive strength: Research on hybrid models genetic based algorithms and ANFIS. Advances in Engineering Software, 67, 156–163. doi:10.1016/j.advengsoft.2013.09.004.

[41] Khursheed, S., Jagan, J., Samui, P., & Kumar, S. (2021). Compressive strength prediction of fly ash concrete by using machine learning techniques. Innovative Infrastructure Solutions, 6(3), 149. doi:10.1007/s41062-021-00506-z.

[42] Hansen, T. C. (1990). Long-term strength of high fly ash concretes. Cement and Concrete Research, 20(2), 193–196. doi:10.1016/0008-8846(90)90071-5.

[43] Mehta, P. K., & Gjørv, O. E. (1982). Properties of Portland cement concrete containing fly ash and condensed silica-fume. Cement and Concrete Research, 12(5), 587–595. doi:10.1016/0008-8846(82)90019-9.

[44] Ravina, D., & Mehta, P. K. (1988). Compressive strength of low cement/high fly ash concrete. Cement and Concrete Research, 18(4), 571–583. doi:10.1016/0008-8846(88)90050-6.

[45] Thomas, M. D. A., & Matthews, J. D. (1992). Carbonation of fly ash concrete. Magazine of Concrete Research, 44(160), 217–228. doi:10.1680/macr.1992.44.160.217.

[46] Lam, L., Wong, Y. L., & Poon, C. S. (1998). Effect of fly ash and silica fume on compressive and fracture behaviors of concrete. Cement and Concrete Research, 28(2), 271–283. doi:10.1016/S0008-8846(97)00269-X.

[47] Atiş, C. D. (2003). High-volume fly ash concrete with high strength and low drying shrinkage. Journal of materials in civil engineering, 15(2), 153-156. doi:10.1061/(asce)0899-1561(2003)15:2(153).

[48] Oner, A., Akyuz, S., & Yildiz, R. (2005). An experimental study on strength development of concrete containing fly ash and optimum usage of fly ash in concrete. Cement and Concrete Research, 35(6), 1165–1171. doi:10.1016/j.cemconres.2004.09.031.

[49] Chalee, W., Ausapanit, P., & Jaturapitakkul, C. (2010). Utilization of fly ash concrete in marine environment for long term design life analysis. Materials and Design, 31(3), 1242–1249. doi:10.1016/j.matdes.2009.09.024.

[50] Liu, M., & Wang, Y. (2011). Prediction of the strength development of fly ash concrete. Advanced Materials Research, 150–151, 1026–1033. doi:10.4028/www.scientific.net/AMR.150-151.1026.

[51] Raja, R., Vijayan, P., & Kumar, S. (2022). Durability studies on fly-ash based laterized concrete: A cleaner production perspective to supplement laterite scraps and manufactured sand as fine aggregates. Journal of Cleaner Production, 366, 132908. doi:10.1016/j.jclepro.2022.132908.

[52] Abhilash, P. T., Satyanarayana, P. V. V., & Tharani, K. (2021). Prediction of compressive strength of roller compacted concrete using regression analysis and artificial neural networks. Innovative Infrastructure Solutions, 6, 1-9. doi:10.1007/s41062-021-00590-1.

[53] Pérez-Acebo, H., Montes-Redondo, M., Appelt, A., & Findley, D. J. (2022). A simplified skid resistance predicting model for a freeway network to be used in a pavement management system. International Journal of Pavement Engineering. doi:10.1080/10298436.2021.2020266.

[54] ASTM C39/C39M-14. (2014). Standard Test Method for Compressive Strength of Cylindrical Concrete Specimens. ASTM International, Pennsylvania, United States. doi:10.1520/C0039M-C0039-14..

[55] ASTM C618-19. (2019). Standard Specification for Coal Fly Ash and Raw or Calcined Natural Pozzolan for Use in Concrete. ASTM International, Pennsylvania, United States. doi:10.1520/C0618-19.

[56] ISO 14067:2018 (2018). Greenhouse gases — Carbon footprint of products — Requirements and guidelines for quantification and communication. International Organization for Standards (ISO), Geneva, Switzerland.

[57] Onyelowe, K. C., Ebid, A. M., Riofrio, A., Soleymani, A., Baykara, H., Kontoni, D. P. N., Mahdi, H. A., & Jahangir, H. (2022). Global warming potential-based life cycle assessment and optimization of the compressive strength of fly ash-silica fume concrete; environmental impact consideration. Frontiers in Built Environment, 8, 992552. doi:10.3389/fbuil.2022.992552.

[58] Onyelowe, K. C., Gnananandarao, T., Ebid, A. M., Mahdi, H. A., Razzaghian Ghadikolaee, M., & Al-Ajamee, M. (2022). Evaluating the Compressive Strength of Recycled Aggregate Concrete Using Novel Artificial Neural Network. Civil Engineering Journal (Iran), 8(8), 1679–1693. doi:10.28991/CEJ-2022-08-08-011.

[59] Onyelowe, K. C., Ebid, A. M., Riofrio, A., Baykara, H., Soleymani, A., Mahdi, H. A., Jahangir, H., & Ibe, K. (2022). Multi-Objective Prediction of the Mechanical Properties and Environmental Impact Appraisals of Self-Healing Concrete for Sustainable Structures. Sustainability (Switzerland), 14(15). doi:10.3390/su14159573.

[60] Onyelowe, K. C., Kontoni, D. P. N., Ebid, A. M., Dabbaghi, F., Soleymani, A., Jahangir, H., & Nehdi, M. L. (2022). Multi-Objective Optimization of Sustainable Concrete Containing Fly Ash Based on Environmental and Mechanical Considerations. Buildings, 12(7), 948. doi:10.3390/buildings12070948.

[61] Ebid, A. M. (2020). 35 Years of (AI) in Geotechnical Engineering: State of the Art. Geotechnical and Geological Engineering, 39(2), 637–690. doi:10.1007/s10706-020-01536-7.

Appendix I

Table A- 1. Utilized computed database

FA/B	FAg/B	CAg/B	Fc28 (MPa)	P
		Training set		
0.30	1.36	2.93	34.5	5.3
0.13	0.62	1.35	42.5	9.5
0.13	2.83	1.30	27.1	4.9
0.37	1.48	0.68	33.6	8.3
0.13	0.70	1.07	36.9	9.8
0.50	2.67	3.71	8.5	4.0
0.13	0.59	1.54	41.1	9.0
0.47	1.13	2.79	25.4	6.0
0.25	0.87	1.82	41.7	7.9
0.30	0.84	2.08	53.0	7.4
0.50	1.13	2.68	33.0	6.1
0.37	1.24	0.57	39.5	9.4
0.58	1.52	3.48	13.4	5.0
0.50	0.71	1.84	48.0	8.5
0.20	2.53	1.16	29.2	5.5
0.20	0.45	1.98	27.7	8.8
0.13	0.59	0.89	42.0	11.0
0.61	1.64	3.67	10.5	4.7
0.25	2.93	1.34	22.9	4.9
0.30	1.09	2.39	45.5	6.4
0.10	0.45	1.98	38.2	8.5
0.50	0.83	1.24	20.9	8.8
0.30	1.09	2.39	47.0	6.4
0.34	2.73	3.77	11.9	3.8
0.30	1.36	2.93	33.5	5.3
0.24	1.38	1.72	43.7	6.9
0.13	3.50	1.60	21.3	4.2
0.15	0.83	1.24	19.9	8.0
0.15	0.95	2.24	50.0	6.7
0.13	0.67	1.44	40.7	9.0
0.13	0.62	1.41	43.6	9.3
0.43	2.67	3.66	7.4	4.0
0.50	2.67	3.68	5.8	4.0
0.25	1.61	0.73	42.5	7.8
0.45	0.83	1.82	35.6	8.6
0.15	0.83	1.31	32.0	8.3
0.13	0.69	1.48	38.9	8.8
0.54	1.39	3.24	17.1	5.3
0.13	0.57	1.06	43.9	10.5
0.33	1.98	0.91	28.5	6.7
0.37	2.34	1.07	20.0	5.9
0.34	2.72	3.74	8.8	3.9
0.20	2.09	0.96	35.6	6.3
0.55	0.81	1.82	24.0	8.9
0.13	0.57	1.26	48.4	10.0
0.50	0.83	1.32	38.8	9.0
0.13	0.51	0.96	47.9	11.2
0.13	0.68	1.05	37.7	9.9
0.13	0.68	1.46	40.3	8.9
0.30	1.45	0.66	42.7	8.4
0.30	0.45	1.98	22.5	9.0
0.25	0.83	1.29	30.3	8.4
0.30	1.73	0.79	36.5	7.4
0.50	0.83	1.16	16.6	8.6

0.13	0.53	1.41	46.1	9.7
0.60	1.67	2.60	10.1	5.8
0.13	0.63	0.99	40.3	10.4
0.43	2.68	3.71	10.4	3.9
0.64	1.75	3.84	8.4	4.5
0.33	1.34	0.61	41.2	8.9
0.33	1.61	0.74	35.5	7.8
0.20	3.15	1.44	22.4	4.6
0.50	0.92	2.11	41.5	7.4
0.13	0.53	1.41	47.3	9.7
0.33	2.50	1.14	21.4	5.6
0.37	1.84	0.84	26.9	7.1
0.13	0.74	1.57	37.2	8.4
0.35	0.83	1.35	45.0	8.8
0.30	0.84	2.08	50.5	7.4
0.13	0.63	1.15	39.9	9.9
0.13	0.62	1.35	43.1	9.5
0.14	1.95	0.89	39.3	6.6
0.35	0.83	1.19	19.9	8.3
0.60	1.67	2.60	9.6	5.8
0.13	2.35	1.08	33.0	5.7
0.13	0.75	1.14	35.2	9.3
0.30	2.68	1.23	22.7	5.3
0.15	1.53	3.15	33.0	4.8
0.29	2.15	0.99	29.8	6.3
0.25	2.33	1.06	29.6	5.9
0.34	2.72	3.75	9.6	3.8
0.13	0.57	1.26	47.3	10.0
0.15	0.83	1.39	47.4	8.5
0.30	0.84	2.08	50.5	7.4
0.50	2.67	3.68	6.1	4.0
0.13	0.60	1.55	39.0	8.9
0.43	2.65	3.66	7.9	4.0
0.25	0.83	1.22	21.0	8.2
0.13	0.69	1.48	38.4	8.8
0.20	1.75	0.80	41.4	7.3
Validation set				
0.30	1.09	2.39	49.5	6.4
0.34	2.73	3.77	12.5	3.8
0.13	0.58	1.07	43.2	10.5
0.30	1.36	2.93	33.5	5.3
0.70	0.93	1.98	30.6	8.2
0.15	0.89	1.82	48.9	7.6
0.25	1.90	0.87	36.2	6.9
0.51	1.88	2.83	13.1	5.2
0.35	0.83	1.27	32.7	8.6
0.51	1.88	2.83	11.2	5.2
0.22	2.25	2.38	23.2	4.7
0.13	0.68	1.46	39.6	8.9
0.13	0.64	1.41	44.0	9.2
0.43	2.68	3.71	9.0	4.0
0.50	0.93	1.98	66.5	8.0
0.13	0.53	1.41	45.1	9.6
0.13	0.64	1.17	38.9	9.8
0.33	1.03	1.58	54.3	8.1
0.50	2.67	3.71	7.3	4.0
0.25	0.83	1.37	43.2	8.6
0.40	0.45	1.98	21.6	9.3
0.15	1.24	2.55	44.5	5.8